



## Why Do Red Blood Cells Have Asymmetric Shapes Even in a Symmetric Flow?

Badr Kaoui,<sup>1,2</sup> George Biros,<sup>3</sup> and Chaouqi Misbah<sup>1</sup>

<sup>1</sup>*Laboratoire de Spectrométrie Physique, UMR, 140 avenue de la physique, Université Joseph Fourier Grenoble, and CNRS, 38402 Saint Martin d'Herès, France*

<sup>2</sup>*Université Hassan II - Mohammedia, Faculté des Sciences Ben M'Sik, Laboratoire de Physique de la Matière Condensée, BP 7955, 20800 Casablanca, Morocco*

<sup>3</sup>*Georgia Institute of Technology, 1324 Klaus Advanced Computing Building, 266 Ferst Drive, Atlanta, Georgia 30332-0765, USA*

(Received 17 July 2009; published 26 October 2009)

Understanding why red blood cells (RBCs) move with an asymmetric shape (slipperlike shape) in small blood vessels is a long-standing puzzle in blood circulatory research. By considering a vesicle (a model system for RBCs), we discovered that the slipper shape results from a loss in stability of the symmetric shape. It is shown that the adoption of a slipper shape causes a significant decrease in the velocity difference between the cell and the imposed flow, thus providing higher flow efficiency for RBCs. Higher membrane rigidity leads to a dramatic change in the slipper morphology, thus offering a potential diagnostic tool for cell pathologies.

DOI: 10.1103/PhysRevLett.103.188101

PACS numbers: 87.16.D-, 83.50.Ha, 83.80.Lz, 87.19.rh

*Introduction.*—Blood is a complex fluid that is primarily composed of red blood cells (RBCs), which occupy (in a healthy human body) about 45% of the blood volume. The rest consists of plasma, while the other blood elements (white blood cells, platelets, etc.) take up less than 1% of the total blood volume.

Because blood is a complex fluid, descriptions of its flow properties escape the traditional laws for simple fluids. The complex character results from an intimate coupling between the shape of RBCs and the ambient plasma, which leads to a rich set of RBC morphologies in the blood circulatory system. Understanding the selection of shapes and dynamics among a large manifold of possibilities is a challenging problem. This type of complexity is a characteristic property of nonequilibrium dissipative systems for which general thermodynamic principles, such as minimization of energy, maximization of entropy, etc., cannot be applied.

At equilibrium (i.e., in a quiescent fluid), healthy RBCs have a biconcave shape that corresponds to a minimal membrane bending energy. Under nonequilibrium conditions, as experienced in a simple shear flow, RBCs reveal a number of interesting shapes and dynamics. The most classical ones are tank-treading ellipsoids [1] (the cell elongates as an ellipsoid and orients itself with a fixed direction, while the fluid membrane shows a tank-treadlike motion) and tumbling motions [2]. These features, among others, are shared with phospholipid vesicles.

In a parabolic distribution of the velocity field (e.g., Poiseuille flow), a situation that is relevant for the blood circulatory system, RBCs assume a parachutelike shape. A clear distinction must be made between a symmetric shape, hereafter simply called a *parachute*, and an asymmetric one, referred to as a *slipper*. The reasons of why RBCs often show asymmetric shapes in a symmetric tube are a puzzle in blood microcirculatory research [3]. Earlier nu-

merical studies reported on a manifestation of these slipper shapes [4,5]. The existence of the slipper has been linked with (i) confinement, and (ii) RBC elasticity (associated with the cytoskeleton a cross-linked network of proteins lying beneath the RBC membrane).

Elucidating the basic relevant mechanisms that are responsible for manifesting the slipper shape is highly desirable. The following questions represent the motivations for this study: (i) Is confinement relevant? (ii) Does the cytoskeleton play a necessary role in the development of the slipper? (iii) How does the slipper occur? And (iv) why does the slipper occur? These constitute questions of primary importance that we would like to address in this Letter.

We focus on the simplest configuration with the aim of identifying the minimal ingredients that are needed for the slipper shape. We consider a purely phospholipid membrane, known as a giant vesicle [6]. This allows us to shed light on whether or not the cytoskeleton is essential. Vesicles and RBCs both have inextensible membranes and exhibit bending modes of the same order of magnitude. The main difference is that RBCs are endowed with an in-plane shear elasticity by virtue of their cytoskeletons. We also disregard the presence of lateral walls, as we neglect confinement. In reality, a Poiseuille flow is bounded by walls (for a real system we have in mind a weak confinement). We consider a 2D simulation, motivated by the fact that in several circumstances a 2D study [7] captures the 3D results [8,9].

*Model.*—We consider the limit of the vanishing Reynolds number (the Stokes limit) and focus on the situation where the internal fluid has the same viscosity as the ambient fluid. The imposed flow reads

$$\mathbf{v}^\infty = v_{\max} \left[ 1 - \left( \frac{y}{W} \right)^2 \right] \mathbf{e}_x, \quad (1)$$

where  $C \equiv 2v_{\max}/W^2$  is the curvature of the flow and must be compared to the typical vesicle radius  $R_0$ . Since here we disregard confinement only  $C$  has a physical meaning.

Vesicle dynamics is formulated using a boundary integral formulation [10,11], in which we express the velocity at a point on the membrane as

$$\mathbf{v}(\mathbf{x}_0) = \mathbf{v}^\infty(\mathbf{x}_0) + \frac{1}{\eta} \oint \mathbf{G}(\mathbf{x} - \mathbf{x}_0) \cdot \mathbf{f}(\mathbf{x}) ds, \quad (2)$$

where the integral is performed along the membrane,

$$G_{ij}(\mathbf{x} - \mathbf{x}_0) = -\delta_{ij} \ln|\mathbf{x} - \mathbf{x}_0| + \frac{(\mathbf{x} - \mathbf{x}_0)_i(\mathbf{x} - \mathbf{x}_0)_j}{|\mathbf{x} - \mathbf{x}_0|^2},$$

is the free-space two dimensional Greens function (or Oseen tensor) for the Stokes operator [12], and  $\eta$  is the dynamic fluid viscosity.  $\mathbf{x}$  and  $\mathbf{x}_0$  are 2D vector positions of a membrane point, and  $\mathbf{f}$  is the membrane force per unit area, given by

$$\mathbf{f} = \kappa \left[ \frac{d^2 c}{ds^2} + \frac{1}{2} c^3 \right] \mathbf{n} - \zeta c \mathbf{n} + \frac{d\zeta}{ds} \mathbf{t}. \quad (3)$$

This force balances the hydrodynamic force jump across the vesicle membrane. This force (derived in 2D in Refs. [7,13]) is obtained from the functional derivative of the Helfrich [14] bending energy  $E = \frac{\kappa}{2} \oint c^2 ds + \oint \zeta ds$ , which includes the local arclength conservation constraint (expressing inextensibility) represented by the Lagrange multiplier  $\zeta$ , the membrane curvature  $c$ , the unit normal and tangent vectors  $\mathbf{n}$  and  $\mathbf{t}$ , the arclength coordinate  $s$ , and the membrane bending rigidity  $\kappa$ . Equation (2) is solved numerically (see [15,16]).

**Results.**—Length is measured in units of the vesicle radius  $R_0$  (defined as the radius of a circle having the same enclosed area). The first dimensionless number that can be formed is  $C_a = \eta v_{\max} R^2 / \kappa$  (or  $\eta C R^4 / \kappa$  if we use  $C$ , the only parameter characterizing the flow in an unbounded geometry). The vesicle deflation is defined as the ratio of the actual enclosed area over the area of a circle having the same perimeter  $p$ :

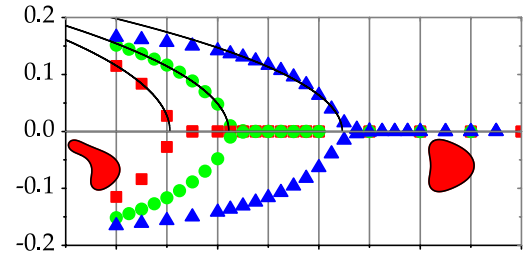
$$\nu = \frac{A}{\pi[p/2\pi]^2}, \quad (4)$$

where  $\nu = 1$  for a circle, and  $0 < \nu < 1$  otherwise. Thus, we have two dimensionless parameters  $\nu$  and  $C_a$ . We also use physical units in our discussion in order to highlight the feasibility of experimental investigations and the connections to blood flow data. We postpone a detailed discussion of the results in a dimensionless form for future work. We have fixed the parameters associated with the imposed Poiseuille flow ( $v_{\max}$  and  $W$ ) and have varied  $\nu$ . For definiteness, we first set  $v_{\max} = 800 \mu\text{m/s}$  (a typical value in human venules [2]) and  $W = 10R_0$ , while  $\eta$  is fixed to the water viscosity (close to that of the blood plasma), and  $\kappa = 10^{-19} \text{ J}$  (a typical value for vesicles and RBCs [17]). For large enough  $\nu$  ( $\nu > 0.7$ ), we have found that vesicles that were initially placed off-center in the Poiseuille flow migrate towards the center, in accord with prior results

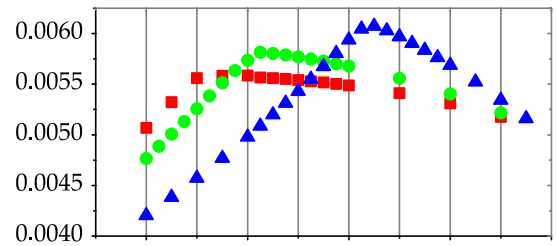
[7,8]. At the center line, the vesicle assumes a parachute (symmetric) shape. This shape is stable against various perturbations. An interesting outcome is that below a critical value of  $\nu = \nu_c \approx 0.7$ , the parachute shape develops an instability that is characterized by the loss of up-down symmetry. The resulting shape is called a *slipper* (see movies in [18]).

We have analyzed, in some detail, the occurrence of this instability. We characterize this symmetry-breaking behavior using the  $y$  position of the center of mass, denoted as  $Y_G$ . For  $\nu > \nu_c$ , the shape is symmetric, and hence  $Y_G = 0$ . For  $\nu < \nu_c$ ,  $Y_G$  acquires a nonzero value. The results are reported in Fig. 1. Because of the symmetry, the  $\pm Y_G$  solutions are equivalent, as checked numerically for sev-

Equilibrium Lateral Position



Slip Velocity



Steady Tank-treading Velocity

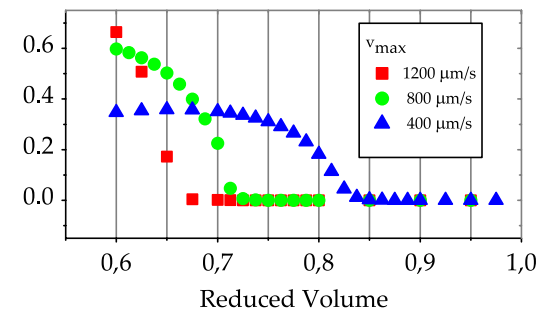


FIG. 1 (color online). Top panel: The behavior of the equilibrium lateral position of the center of mass  $Y_G$  as a function of  $\nu$  for different values of the flow parameter  $v_{\max}$ . The full lines are fits with  $(\nu_c - \nu)^{1/2}$ . Middle panel: The slip velocity (normalized by  $v_{\max}$ ) as a function of  $\nu$ . The slip velocity (or lag) is defined as the difference between the vesicle (when its vertical position has reached a plateau with time) and the corresponding unperturbed velocity at the position of the vesicle center of mass ( $Y_G = 0$  for the parachute shape, and  $Y_G \neq 0$  for the slipper). Bottom panel: The tank-treading velocity. The link with physical units is explained in the discussion.

eral cases that we do not report here. We can conclude that the parachute-slipper transition corresponds to a supercritical bifurcation (the dynamical analogue of a second order phase transition). A fit is shown in Fig. 1 (solid line in the upper panel), and we find that in the vicinity of the bifurcation point  $Y_G \sim 0$  and for  $\nu < \nu_c$ ,  $Y_G \sim (\nu_c - \nu)^{1/2}$  constitutes a very good approximation. This is the signature of a supercritical (or pitchfork) bifurcation, which belongs to the cusp catastrophe family. For the set of parameters explored so far, we find that the supercritical nature of the bifurcation persists. We cannot, however, exclude the possibility of a subcritical bifurcation (the dynamical analogue of a first order transition, where  $Y_G$  would jump from zero to a finite value at a critical  $\nu$ ) belonging to the butterfly catastrophe family. Our results suggest that  $Y_G$  should obey, in the vicinity of the bifurcation point, an equation of the form

$$\frac{dY_G}{dt} = (\nu_c - \nu)Y_G - Y_G^3. \quad (5)$$

This equation has a trivial fixed point  $Y_G = 0$  for all  $\nu$  and a nontrivial pair of solutions  $Y_G = \pm\sqrt{\nu_c - \nu}$  for  $\nu < \nu_c$ . It is a simple matter to show that  $Y_G = 0$  is stable for  $\nu > \nu_c$  and loses its stability for  $\nu < \nu_c$  in favor of two stable branches  $Y_G = \pm\sqrt{\nu_c - \nu}$ .

Once the question of how the slipper occurs is settled, we are in a position to address the next natural question of why a slipper forms at all. The shear rate is minimal (actually it vanishes) at the center of the Poiseuille flow, and it is expected that any deviation of the vesicle from the center line would be penalized by higher dissipation as a result of the higher shear rate. Furthermore, for a symmetric (parachute) shape, membrane tank-treading is absent because of an obvious central symmetry. As a consequence, the relative velocity of the fluid inside the parachute vanishes. A slipper shape is accompanied by a tank-treading membrane, and thus by flow circulation inside the cell. Because of the presence of this additional flow, one would expect higher dissipation, and from this point of view a slipper should not be favored.

In fact, we find that a key property that dictates the establishment of a slipper is associated with the notion of lag between the vesicle and the imposed flow (i.e., the difference between the vesicle velocity and that of the bare imposed flow). One outcome of our study (Fig. 1, middle panel) is that the lag increases with decreasing  $\nu$  and attains a maximum (within numerical uncertainties) at the bifurcation point, where the manifestation of a slipper is accompanied by a decrease in the lag. This feature has been found for every parameter explored so far. By assuming an asymmetric shape, the vesicle reduces its lag, albeit at the price of inducing membrane tank-treading and internal flow. The reduction of lag occurs as a subtle interplay between the shape adaptation to the flow and a compromise between additional membrane and vesicle internal dissipation. As a consequence, the slipper becomes a favorable shape.

We have performed a systematic study to determine the boundary in parameter space that separates the parachute shape from the slipper one. In this brief exploration, we keep the membrane bending rigidity fixed to a typical value for vesicles used above and vary both the flow strength, measured by  $\nu_{\max}$ , and the degree of deflation  $\nu$ . The results are shown in Fig. 2. There, we also show a panel of shapes that are exhibited as a function of the flow and deflation conditions. The slipper takes place in the yellow region, while the parachute shape prevails in the violet one. It was also useful to distinguish between a parachute with a negative curvature at the rear and one with a positive curvature (renamed a *bullet*).

Finally, we studied the evolution of the slipper shape as a function of the membrane rigidity, for fixed  $\nu_{\max}$ ,  $W$ , and  $\nu$ . We found a dramatic change in the morphology, even when the rigidity increases by a factor of 2 only. Figure 3 shows the results. Several RBC pathologies, such as malaria, are accompanied by an increase in the elastic membrane modulus. Exported proteins from parasites cause a significant increase in membrane rigidity, which may attain values that are 2.6 times higher than those of uninfected RBCs [19]. This result, after adequate refinement that includes shear elasticity and lateral walls, may be used as a potential diagnostic for detecting RBC pathologies. Multilayer vesicles, as well as polymer-decorated membranes, exhibit higher rigidity, thus offering a model system on which to directly test the present findings in a weakly confined channel.

*Discussion.*—Vesicles and RBCs exhibit both membrane inextensibility and bending modes. Membrane bending

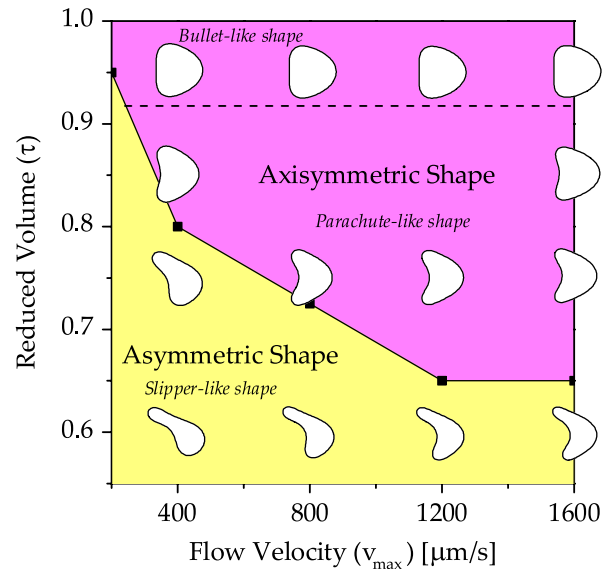


FIG. 2 (color online). Phase diagram in the plane of reduced volume and maximum imposed velocity. Evolution of the shapes is shown. Filled squares represent the boundary of the symmetry-breaking bifurcation, and the solid line is a guide for the eyes. The horizontal dashed line represents the boundary below which the parachute shape has a negative curvature at the rear. Here  $W/R_0 = 10$ .

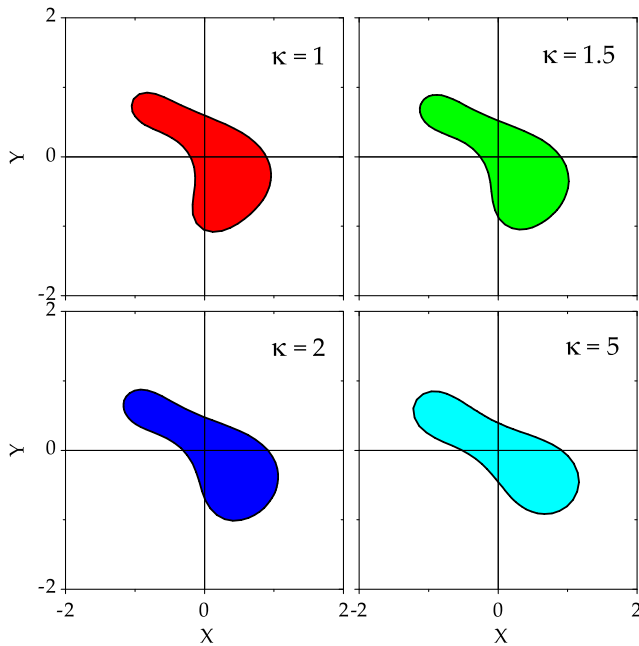


FIG. 3 (color online). Evolution of the morphology of a slipper as a function of membrane rigidity.  $\kappa = 1$  refers to the typical value  $10^{-19}$  J for vesicles and RBCs. Here we have taken reference values (typical in venules), namely  $V_{\max} = 800 \mu\text{m/s}$  and  $W/R_0 = 10$ .

rigidity for vesicles is of the order of  $10^{-19}$  J and is close to that of RBCs [17]. Bending under a shear flow with shear rate  $\gamma$  is characterized by the dimensionless number  $C_b = \eta R_0^3 \gamma / \kappa$ . Unlike vesicles, RBCs have an in-plane shear elasticity (as a result of the cytoskeleton). It is characterized by the shear modulus [17]  $\mu_s \sim 2-6 \times 10^{-6}$  N/m [17], and by the dimensionless number  $C_s = \eta R_0 \gamma / \mu_s$ . The ratio between  $C_s$  and  $C_a$  shows that bending and shearing are of the same order. We have disregarded here the shear elasticity. This has allowed us to show that the slipper manifestation is not dictated by the cytoskeleton. Future studies should include shear elasticity and confinement for a quantitative application to RBCs.

For small arteries (with a diameter of about  $100 \mu\text{m}$ ), and venules (with diameters in the  $20 \mu\text{m}$  range) a typical  $v_{\max}$  value falls in the interval between  $10^5 \mu\text{m/s}$  and  $10^4 \mu\text{m/s}$  [2]. Consequently, given the fact that  $\nu \sim 0.65$  for RBCs, slippers (see Fig. 2) are more favorable in venules and capillaries than they are in arteries, a result in agreement with reported experiments [3]. We are not aware of a phase diagram like the one presented in Fig. 2 for vesicles. Thus, this Letter should serve as a guide for future systematic experimental studies on vesicles, which, unlike RBCs, lend themselves to ample variation with respect to their reduced volume. This is an essential step in testing the present findings. It will also be interesting to study the role of confinement on RBCs as reported experimentally [20].

**Conclusion.**—We have shown that a major advantage of the slipper shape is a reduction in the lag (i.e., the slipper

shape enhances transport efficiency). Neither confinement nor membrane shear elasticity seems to be a necessary ingredient [4,5,21]. It is not yet clear whether or not, beyond the transport efficiency found here, the slipper shape is dictated by other physiological determinants. One possibility might be a necessity for the membrane to tank-tread (recall that tank-treading is absent for a symmetric shape) in order to efficiently mix the hemoglobin, and thus, enhance oxygen distribution in tissues.

C.M. benefited from financial support from CNES, ESA, and ANR (MOSICOB), and B.K. from a Volubulus grant. G.B. was partially supported by the U.S. National Science Foundation Grants No. OCI 0749285 and No. CNS-0540302.

- 
- [1] T. Fischer, M Stohr-Lissen, and H Schmid-Schonbein, *Science* **202**, 894 (1978).
  - [2] Y.C. Fung, *Biomechanics* (Springer, New York, 1990).
  - [3] R. Skalak, *Science* **164**, 717 (1969).
  - [4] T.W. Secomb and R. Skalak, *Microvasc. Res.* **24**, 194 (1982).
  - [5] C. Pozrikidis, *Phys. Fluids* **17**, 031503 (2005).
  - [6] *Structure and Dynamics of Membranes, Handbook of Biological Physics*, edited by R. Lipowsky and E. Sackmann (Elsevier, Amsterdam, 1995).
  - [7] B. Kaoui, G.H. Ristow, I. Cantat, C. Misbah, and W. Zimmermann, *Phys. Rev. E* **77**, 021903 (2008).
  - [8] G. Danker, P.M. Vlahovhska, and C. Misbah, *Phys. Rev. Lett.* **102**, 148102 (2009).
  - [9] G. Coupier, B. Kaoui, T. Podgorski and C. Misbah, *Phys. Fluids* **20**, 111702 (2008).
  - [10] M. Kraus, W. Wintz, U. Seifert, and R. Lipowsky, *Phys. Rev. Lett.* **77**, 3685 (1996).
  - [11] I. Cantat and C. Misbah, *Phys. Rev. Lett.* **83**, 235 (1999).
  - [12] C. Pozrikidis, *Boundary Integral and Singularity Methods for Linearized Viscous Flow* (Cambridge University Press, Cambridge, England, 1992).
  - [13] I. Cantat, Ph.D. thesis, University J. Fourier, Grenoble I, France, 1999.
  - [14] Ou-Yang Zhong-can and W. Helfrich, *Phys. Rev. A* **39**, 5280 (1989).
  - [15] I. Cantat, K. Kassner and C. Misbah, *Eur. Phys. J. E* **10**, 175 (2003).
  - [16] S.K. Veerapaneni, D. Gueyffier, D. Zorin, and G. Biros, *J. Comput. Phys.* **228**, 2334 (2009).
  - [17] N. Mohandas and E. Evans, *Annu. Rev. Biophys. Biomol. Struct.* **23**, 787 (1994); L. Scheffer, A. Bitler, E. Ben-Jacob, and R. Korenstein, *Eur. Biophys. J.* **30**, 83 (2001).
  - [18] See EPAPS Document No. E-PRLTAO-103-004942 for movies. For more information on EPAPS, see <http://www.aip.org/pubservs/epaps.html>.
  - [19] S. Suresh, *J. Mater. Res.* **21**, 1871 (2006).
  - [20] M. Abkarian, M. Faivre, R. Horton, K. Smistrup, C. A. Best-Popescu, and H. A. Stone, *Biomedical Materials* **3**, 034011 (2008).
  - [21] H. Noguchi and G. Gompper, *Proc. Natl. Acad. Sci. U.S.A.* **102**, 14 159 (2005).